SANDIA REPORT
SAND2004-6612
Unlimited Release
Printed January 2005

LDRD Final Report on Engineered Superconductivity in Electron-hole Bilayers

M.P. Lilly, E. Bielejec, J.A. Seamons, D.R. Tibbetts, R.G. Dunn, S.K. Lyo, J.L. Reno, L. Stephenson, W.E. Baca, J.A. Simmons

Prepared by
Sandia National Laboratories
Albuquerque, New Mexico 87185 and Livermore, California 94550

Sandia is a multiprogram laboratory operated by Sandia Corporation,
a Lockheed Martin Company, for the United States Department of Energy's
National Nuclear Security Administration under Contract DE-AC04-94AL85000.

Approved for public release; further dissemination unlimited.

Issued by Sandia National Laboratories, operated for the United States Department of Energy by Sandia Corporation.

NOTICE: This report was prepared as an account of work sponsored by an agency of the United States Government. Neither the United States Government, nor any agency thereof, nor any of their employees, nor any of their contractors, subcontractors, or their employees, make any warranty, express or implied, or assume any legal liability or responsibility for the accuracy, completeness, or usefulness of any information, apparatus, product, or process disclosed, or represent that its use would not infringe privately owned rights. Reference herein to any specific commercial product, process, or service by trade name, trademark, manufacturer, or otherwise, does not necessarily constitute or imply its endorsement, recommendation, or favoring by the United States Government, any agency thereof, or any of their contractors or subcontractors. The views and opinions expressed herein do not necessarily state or reflect those of the United States Government, any agency thereof, or any of their contractors.

Printed in the United States of America. This report has been reproduced directly from the best available copy.

Available to DOE and DOE contractors from
U.S. Department of Energy
Office of Scientific and Technical Information
P.O. Box 62
Oak Ridge, TN 37831

Telephone: (865)576-8401
Facsimile: (865)576-5728
E-Mail: reports@adonis.osti.gov
Online ordering: http://www.osti.gov/bridge

Available to the public from
U.S. Department of Commerce
National Technical Information Service
5285 Port Royal Rd
Springfield, VA 22161

Telephone: (800)553-6847
Facsimile: (703)605-6900
E-Mail: orders@ntis.fedworld.gov
Online order: http://www.ntis.gov/help/ordermethods.asp?loc=7-4-0#online

SAND2004-6612
Unlimited Release
Printed January 2005

LDRD final report on engineered superconductivity in electron-hole bilayers

M. P. Lilly, E. Bielejec, J. A. Seamons, D. R. Tibbetts, R. G. Dunn, S. K. Lyo, J. L. Reno, L. Stephenson, W. E. Baca, J. A. Simmons
Semiconductor Materials and Device Sciences Department
Sandia National Laboratories
P. O. Box 5800
Albuquerque, NM 87185-1411

Abstract

Macroscopic quantum states such as superconductors, Bose-Einstein condensates and superfluids are some of the most unusual states in nature. In this project, we proposed to design a semiconductor system with a 2D layer of electrons separated from a 2D layer of holes by a narrow (but high) barrier. Under certain conditions, the electrons would pair with the nearby holes and form excitons. At low temperature, these excitons could condense to a macroscopic quantum state either through a Bose-Einstein condensation (for weak exciton interactions) or a BCS transition to a superconductor (for strong exciton interactions). While the theoretical predictions have been around since the 1960's, experimental realization of electron-hole bilayer systems has been extremely difficult due to technical challenges. We identified four characteristics that if successfully incorporated into a device would give the best chances for excitonic condensation to be observed. These characteristics are closely spaced layers, low disorder, low density, and independent contacts to allow transport measurements. We demonstrated each of these characteristics separately, and then incorporated all of them into a single electron-hole bilayer device.

The key to the sample design is using undoped GaAs/AlGaAs heterostructures processed in a field-effect transistor geometry. In such samples, the density of single 2D layers of electrons could be varied from an extremely low value of 2×10^{9} cm^{-2} to high values of 3×10^{11} cm^{-2}. The extreme low values of density that we achieved in single layer 2D electrons allowed us to make important contributions to the problem of the metal insulator transition in two dimensions, while at the same time provided a critical base for understanding low density 2D systems to be used in the electron-hole bilayer experiments. In this report, we describe the processing advances to fabricate single and double layer undoped samples, the low density results on single layers, and evidence for gateable undoped bilayers.

Intentionally left blank

Table of Contents

Abstract 3
Table of Contents 4
Accomplishments 6
    Undoped heterostructure fabrication 7
    Low density 2D systems: metallic and insulating properties 11
    Undoped electron-electron bilayers 15
    Prospects for electron-hole bilayers and exciton condensation 17
Appendix I: List of refereed publications and presentations 18
    Publications 18
    Invited Presentations 18
Initial Distribution 20

Accomplishments

Excitonic condensation of electron-hole systems has been sought after for over 20 years now. During this time, many different material systems have been considered and studied as a base system for creating the electron-hole system. Examples include excitons at CuO_2 surfaces, polaritons, optically generated electrons and holes in quantum wells and various III-V semiconductor systems. Problems include short lifetimes leading to non-equilibrium and thermal issues, tunneling between layers preventing condensation, and lack of clear experimental techniques to fully exhibit the underlying physics. Clearly this is an extraordinarily difficult problem. Our approach to fabricating electron-hole bilayers has been to use a well known and well understood platform for making 2D systems (GaAs heterostructures), and engineering the appropriate conditions to best observed exciton condensation. These conditions are 1) closely spaced electron and hole layers to maximize the exciton binding energy, 2) low density to enhance interlayer interactions, and 3) high mobility to reduce the effect of disorder and allow the macroscopic quantum state to form.

To meet these conditions, we utilize processing techniques where 2D systems can be field-induced in undoped GaAs/AlGaAs heterostructures. While the FET geometry is common in Si semiconductor devices, GaAs devices are typically doped with Si, Be or C and contact is made by annealing metallic alloys to contact the as-grown carrier systems. The drawback to these doping techniques is that utilizing p-type doping *and* maintaining high mobility has been a major materials problem. By using undoped material, carriers can be drawn from *locally* doped regions (i.e. the contacts) with voltages applied to metallic gates. The depending on the polarity of the gate voltage and the type of ohmic contact (n or p), either electrons or holes are possible. The processing technique for forming the contact-gate region usually used for this procedure is called "self-aligned contacts", and was developed by Bruce Kane at Bell Labs in the early 1990's. We have made significant advances to improving the reliability and reproducibility of single 2D layers fabricated with this technique. We have also demonstrated the first completely undoped electron-electron bilayer using a combination of self-aligned contacts and flip-chip thinning (EBASE, developed by Jerry Simmons at Sandia in the mid-1990s). In the first section, the basic processing and all of our advances are described.

Single layer and bilayer devices made using the undoped GaAs heterostructures can be gated to extremely low density. Low density 2D systems are of much interest to the community, both for applied and fundamental reasons. Our basic understanding of transport in 2D has been in question due to the observation of a 2D metal-insulator transition, and the ultra-low density 2D electrons and holes made for this project have significantly impacted this field. On the applied side, grating-gated bilayers biased near depletion can detect terahertz radiation. Understanding the role of density and optimizing THz detector characteristics is one focus of a new 2005 LDRD project at Sandia. In the second and third section of this report, we document experiments that report the electrical characteristic of single layers at very low density (second section) and evidence for undoped electron bilayers (third section).

Finally, in the last section we discuss on-going efforts to fabricate electron-hole bilayers using undoped material, recent experiments on excitonic condensation, and prospects for the novel techniques that have been developed in this LDRD.

Undoped heterostructure fabrication

Develop techniques for reliable fabrication of single 2D layers in undoped heterostructures. Over the course of this project, we have made a number of improvements to the processing of single-layer undoped heterostructures with the goal of increasing the device performance and yield. Reliable techniques for single layer devices are especially important when the more complex bilayer devices are fabricated. The basic operation of the of the undoped GaAs heterostructure is shown in Figure 1. The contact regions form local reservoirs of carriers. When a gate is placed nearby, a voltage on the gate creates a fringing electric field with the contacts, and draws carriers into the channel. Once the 2D system is formed, the density is proportional to the gate voltage. For electrons the n-type ohmics are NiGeAuNiAu, and a positive voltage induces the 2D electron gas (2DEG). For holes, the ohmic metal is AuBe and a negative voltage is required.

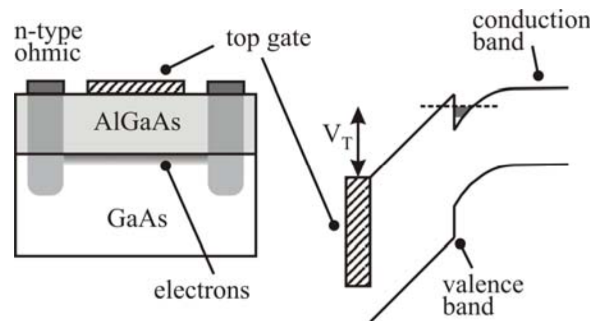

Figure 1. Schematic diagram of a single layer undoped heterostructure

Processing is critical in these devices, and there are a number of common failures. First, the gate (an n+ cap on the structure) must be contacted with a shallow contact. If the gate contact anneals too deep it shorts to the 2DEG; some materials that do not penetrate deep in the sample lead to high resistance contacts (e.g. CrAu). The second common problem is the contact is too close to the gate and the ohmic contact shorts. This often occurs randomly with AuNiGe since it has a bumpy morphology after annealing. A few contacts that short can often be scratched off of the sample. The third problem (and the one we faced most frequently) is that the ohmic contact is too far from the gate. In the mild case, the 2DEG forms but with very high contact resistance. In the severe case, no 2DEG forms at all.

The most straightforward advance we made to processing samples was to change the gate contact metal. Previously unalloyed AlCr was used to contact the n+ layer. The advantage of a such a contact is that the gate and the 2D system cannot be shorted during the anneal process. The drawback is the large contact resistance and frequently failure to contact the n+ at all. We have replaced the AlCr with an alloy of PdGeAu. This new alloy can be annealed at low temperature, has a very low contact resistance, does not short to the 2D layer and always works.

During this project, most of the struggles occurred in finding the optimal method for creating the self-aligned ohmic contact. We found several solutions to putting the contacts where we wanted, and unfortunately, every new wafer design we tested required a custom process for making self-aligned ohmic contacts. The most important step was to find a way to move the ohmic metal closer to the gate, but not so close that electrical connection between the gate and the contact is established. In all cases, the contact location was etched before the ohmic metal was deposited. This etched pit served to displace the ohmic both laterally and vertically. Two techniques were developed to accomplish the lateral control required. The first is evaporating the contact at an angle shown schematically in Figure 2 in order to move the contact closer to the gate beyond the photoresist overhang. Obviously, the deposition must be the same all around the sample, so the actual process is to evaporate the NiGeAu alloy at an angle while rotating the sample to maintain uniformity. This process results in lower contact resistances, and more importantly, provides a mechanism to tune distance from the contact to the gate by changing the angle of evaporation. For samples 600 nm below the surface, this technique make contacts with very low resistance, but the yield is low. For samples with the 2DEG 200 nm below the surface, this technique is very reliable.

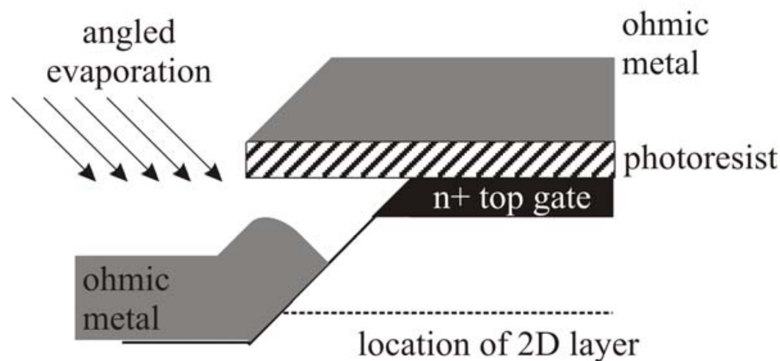

Figure 2. Evaporating the ohmic contact at an angle lowers the contact resistance by depositing the metal closer to the gate.

A second method to control the lateral displacement from the contact to the gate is to use a combination of anisotropic and isotropic etching before ohmic metal deposition. The first etch is an anistropic etch with vertical sidewalls. This creates depth without moving the contact too far away. The second etch is a wet etch that both etches laterally and vertically. Varying the ratio allows any combination of total depth and lateral displacement. A cross-section scanning electron microscope image of a sample etched in this manner is shown in Figure 3. This technique make both low resistance contacts with a high yield (near 80% for 2DEGs 600 nm below the surface).

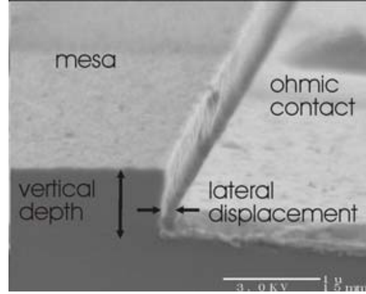

Figure 3. SEM cross section view of a self-aligned ohmic contact fabricated using a combination dry and wet etch.

Fabricate both n-type and p-type single layers. Using undoped heterostructures grown at Sandia, we have achieved single 2D layers of electrons and holes with high mobility. For the n-type sample, the density can be adjusted over a range of more than an order of magnitude with a lower limit of 5×10^{9} cm^{-2}. The mobility, shown in Figure 4, is high throughout the entire density range, with a peak mobility of close to 3 million. Similar results have been found for 2D holes The low electron and hole densities and corresponding high mobilities made possible by this technique are critical for bilayer experiments. In material supplied by L. N. Pfeiffer at Lucent Technologies, Bell Laboratories, the peak mobility can reach 1.4×10^{7} cm^{2}/Vs.

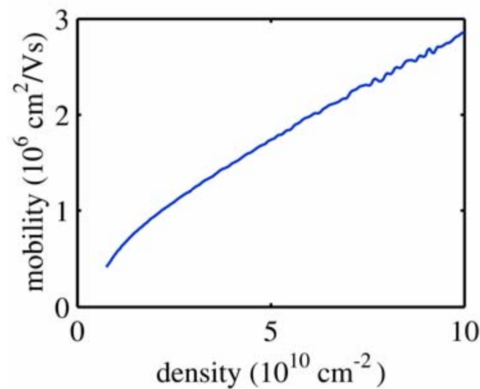

Figure 4. Mobility of a 2D electron system grown and processed at Sandia.

Resistance anisotropy. Our initial resistivity measurements on 2D electron systems at low density $n<10^{10}$ cm^{-2} indicated the presence of a puzzling in-plane resistance anisotropy. In Figure 5a, the 4-wire resistance using contacts at the corners of a 1mm × 1mm square mesa are shown as a function of density. The two curves represent contact configurations such that the current flow vertically (dashed) and horizontally (solid). For an isotropic resistivity in a square geometry, we expect these resistances to be identical. In all of the initial samples fabricated a large anisotropy (up to 30 to 1) was always observed at low density. A systematic study of a number of samples found no correlation between the anisotropy direction and the in-plane crystal directions, as might be expected of an intrinsic anisotropic electron state (such as charge density waves in high Landau levels[1]). We did find, however, that for all of the samples examined, *the*

[1] M. P. Lilly, *et al.*, Phys. Rev. Letters **82**, 394 (1999).

anisotropy was always related to the position of the polyimide bridges located on the surface of the sample. These bridges are shown in the left diagram of Figure 6. This strongly suggests that the anisotropy is an extrinsic effect caused by surface features.

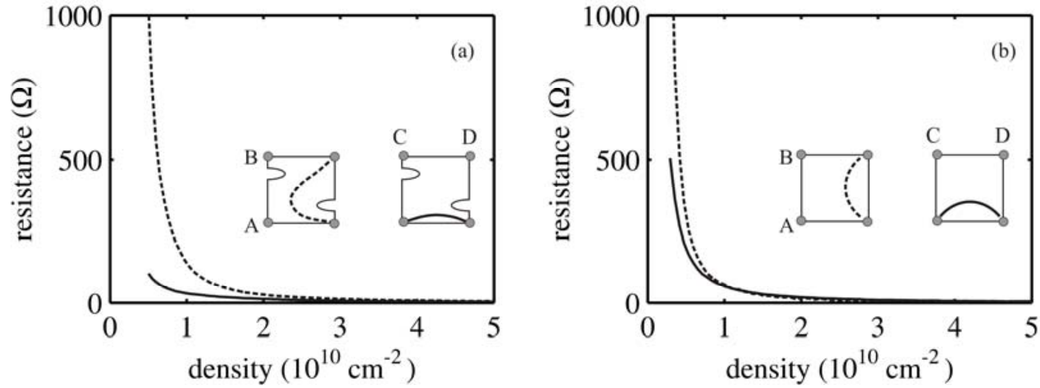

Figure 5. In (a), the first generation of low density devices exhibited an apparent resistance anisotropy. The diagrams indicate current flow. In (b), the new device geometry has a more uniform current flow.

Our speculation is that the polyimide bridges or the gate contacts (CrAl or PdGeAu) locally alter the GaAs heterostructure and slightly lower the density in their vicinity. One possible mechanism is strain. If this occurs, the geometry is no longer square, as indicated in the cartoons in Figure 5a. For current flowing vertically, the current is pushed to the center of the sample and the voltage drop at the opposite corners (A,B) is higher (larger resistance). For current flowing horizontally, the current stay near the edge of the sample, and the other corners (C,D) have a small voltage drop. This effect will be most dramatic when the density is low, since a slight density variation a large change to the geometry. With this hypothesis, we redesigned the device geometry to form the gate contact in a location physically removed from the square region where the resistivity measurements are made (Figure 6, right diagram). The transport results in the new geometry are shown in Fig. 5b. For samples fabricated with the new design, the resistances are much closer.

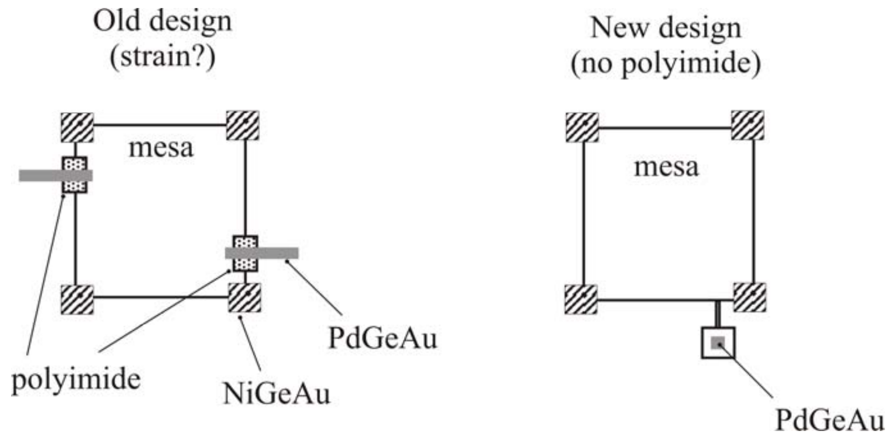

Figure 6. Schematic top view of a square mesa where gate contact might strain the measurement region (left) and where the gate contact is made away from the measurement region (right)

Undoped bilayers. In order to extend the fabrication techniques to undoped bilayer systems, the self-aligned contacts on the surface of the sample must be integrated with the EBASE (epoxy bond and stop etch) technique and back-side processing. With the same processing techniques, electron-electron, hole-hole and electron-hole bilayers can be fabricated. The electron-electron and hole-hole bilayers are relatively straightforward to test. All that is required are top and bottom gate voltages to induce carriers. Transport characterization of an electron-electron bilayer are presented in the third section. Electron-hole bilayers are more complicated, and require an interlayer voltage of approximately the band gap voltage (1.5 volts for GaAs) in addition to top and bottom gate voltages. Our plan for the undoped bilayer allow separate electrical contact to both layers and individual control of the density in each layer. Results from undoped bilayers are presented in the third section of this report.

Low density 2D systems: metallic and insulating properties

In this section, three experimental results on single layer 2D electron systems are presented. First, the density dependence of the resistivity is discussed. These results show that the apparent metallic behavior (drop in resistivity as the temperature is lowered) is a consistent with ionized impurity scattering. Second, weak localization is observed as a negative magnetoresistance feature near zero field. The characteristic log(T) increase in resistance is overwhelmed by ionize impurity scattering effects. Separating the various magnetoresistance contributions to isolate weak localization in this regime is difficult. Finally, the lowest density results are analyzed with density inhomogeneity in mind. A percolation scaling form fits the conductivity very well for both high and low mobility 2DEGs.

Density dependence of the resistivity. The data in Figure 7 show the temperature dependence of the resistivity for an undoped single layer heterojunction. The high density data is characterized by a decreasing resistivity (ρ) as the temperature (T) decreases. In the inset, the inverse mobility (μ^{-1}=n e ρ, where μ is the mobility and n is the density) is linear with T with a slope independent of density; this result is in *quantitative* agreement with acoustic phonon scattering. Over a wide range of intermediate densities a local maximum is observed at low temperature. In this regime, ionized impurity scattering leads to a competition between screening ($\rho \sim T$) for $T<T_F$ and degenerate to non-degenerate Fermi statistics ($\rho \sim T^{-1}$) for $T>T_F$ and causes the formation of the peak. Scattering calculations including phonons and ionized impurities are in excellent qualitative agreement with the data for the intermediate densities. The lowest densities exhibit insulating behavior. The power-law temperature dependence observed here is not consistent with either weak or strong localization, and remains an open question.

This combination of detailed transport measurements and comparison to scattering theory is an important contribution to the 2D metal-insulator transition (MIT) community. Within the standard framework of Fermi liquid theory, a 2D metal-insulator transition is not expected. At low enough temperature, all 2D systems are expected to be insulating. Experimental observations of a metallic regime (decreasing ρ with decreasing T) suggest the possible formation of a novel metallic state. Our work on high mobility 2D electrons shows that the underlying physics is Fermi liquid physics and *not* a new many-body effect.

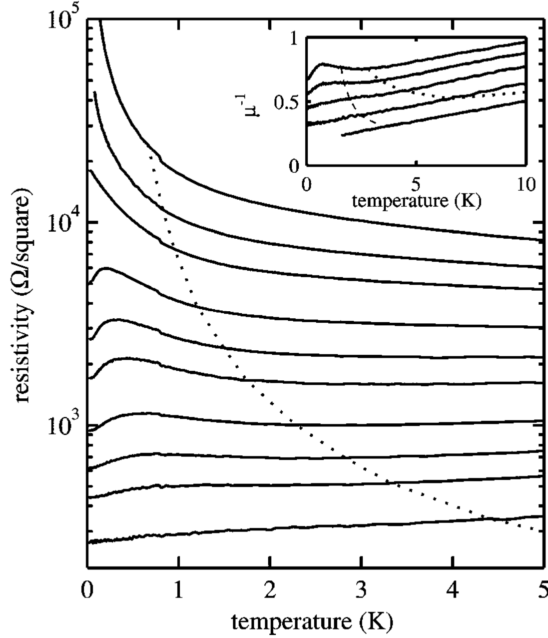

Figure 7. Main figure: resistivity for densities (from the top) 0.16, 0.20, 0.23, 0.29, 0.36, 0.42, 0.55, 0.680.80 and 1.06 x 10^{10} cm^{-2}. The dotted line indicates the Fermi temperature. Inset: inverse mobility for 0.68, 0.80, 1.06, 1.57 and 3.36 x 10^{10} cm^{-2}.

Weak localization phenomena. To observe superconductivity in electron-hole bilayers, interlayer Coulomb correlations must be strong. One way to achieve this is to use low sheet densities, but now so low that the 2D layers become insulating. Due to the unusual insulating behavior mentioned above, we initiated a study of the transport characteristics of a moderate mobility 2D electron system. The low-field magnetoresistance for a 20 μm wide hallbar is shown in Figure 8. For each density and temperature, a clear parabolic background is observed. In addition, a second peak[2] can be discerned in the high density (Figure 8a) and low density data (Figure 8c). The parabolic background is due to an electron-electron interaction correction to the conductivity. The temperature independent peak at high density is due to boundary scattering of quasi-ballistic electrons off of the 20 μm wide mesa edges and can be observed for $T < 5$ K. This effect is only present in high mobility samples where the mean free path of the electron is very long, and the strong signature observed here attests to the high quality of the semiconductor material. The more fragile peak observed at 0.28 K for the low density data (Figure 8c, solid line) has a much different origin. Time-reversed scattering paths have a finite probability of destructive interference, leading to a slightly increased resistivity. This quantum correction to the resistivity is the so-called weak localization effect. The characteristic shape of the weak localization peak (inset, Figure 8c) can be used to extract the electron wavefunction's phase coherent lifetime. This information will be a useful tool for future experiments on electron-hole bilayers where the predicted superconductivity will arise from phase coherent electron-hole pairs. Other than the weak localization correction, the overall resistivity is decreasing as the temperature decreases. The log(T) insulating behavior characteristic of weak localization is not observed in this sample due to the strong ionized impurity scattering temperature dependences.

[2] The peaks occur at an actual field of B=0. The x-axis is non-zero due to trapped flux in the superconducting magnet.

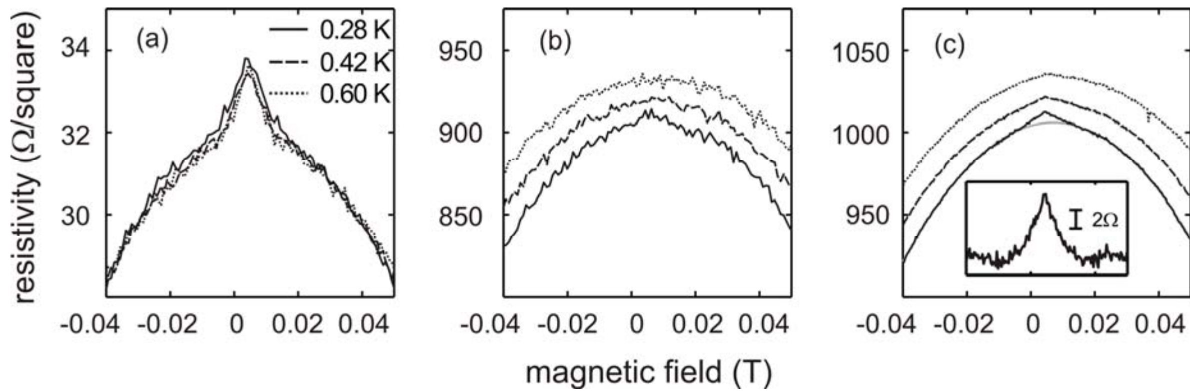

Figure 8. Magnetoresistance for 3 different densities (see panels). Each curve a fixed temperature (see legend in panel a). In (c), the inset shows the weak localization peak after the parabolic background is removed.

Percolation in ultra-low density 2D electrons.

While ionized impurity scattering and weak localization concepts capture the qualitative behavior of the temperature dependence of the resistivity, a complete understanding of the lowest density requires percolation concepts. The basic picture of the percolation transition for 2D MIT is simple and highly physically motivated (Figure 9). As the carrier density n is lowered in a 2D system, screening becomes progressively weaker and strongly nonlinear. A small decrease in n leads to a large decrease in screening, and eventually to a highly inhomogeneous 2D system as the electron gas becomes unable to screen the disorder potential. This gives rise to a random ``hill-and-valley" potential landscape with the 2D carriers repelled from the potential hills and accumulating at the potential valleys. Once these ``depletion zones", associated with the disorder potential hills are numerous enough to prevent conducting paths (Figure 9a) that span the 2D system, an effective 2D MIT transition takes place with the system being an effective metal (insulator) for $n>(<)n_c$ where n_c is the critical percolation density. This percolation picture is particularly germane to 2D semiconductor systems because the disorder potential here arises from the presence of random charged impurities in the system making electronic screening a key ingredient in the effective disorder seen by the carrier system.

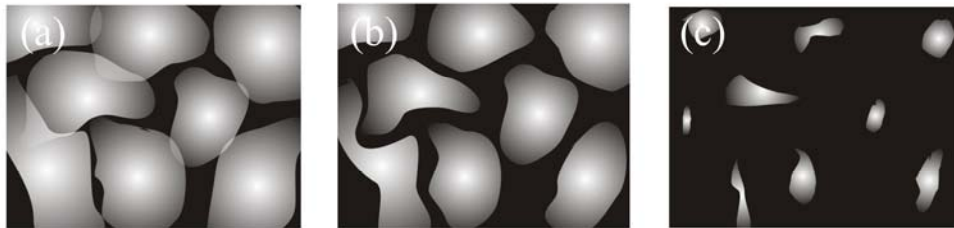

Figure 9. Diagram of inhomogeneous electron density for (a) $n < n_c$, (b) $n \sim n_c$ and (c) $n > n_c$. The black regions represent high electron density, and the white regions have no electrons. Percolation occurs when a finite density electron path spans the 2D system.

The experimentally measured conductivity $\sigma(n)$ is shown in Figure 10 for two samples. Both samples are undoped 2D heterojunctions, with sample A having a higher mobility than sample B.

We first discuss a few salient qualitative features of the density dependent transport properties of our results. At high densities ($n > 10^{10}$ cm^{-2}), the conductivity depends on the density approximately as $\sigma \sim n^{\alpha}$ with α 1.6. This high density behavior is completely consistent with Boltzmann theory based calculations assuming the conductivity being limited by linearly screened charged impurity scattering. As the density decreases, the power α increases rapidly at low density. Although a part of this strong density dependence of $\alpha(n)$ at low density can be understood as arising from the strong suppression in screening at low carrier densities, we find that screening in a *homogeneous* electron gas fails qualitatively in explaining the $\sigma(n)$ behavior at low densities.

In Figure 10, we fit our measured conductivity $\sigma(n)$ to the expected[3] percolation "critical" behavior

$$\sigma(n) = A \cdot (n - n_c)^{\delta}$$

where δ is the conductivity percolation exponent characterizing the vanishing of the conductivity. Fitting the conductivity to Eq. (1) is performed for a range of the low density data. For sample A the data used in the fit is $1\times10^9 < n < 4\times10^9$ cm^{-2}, although the results do not depend sensitively on the exact range of data used in the fit. For Sample B, the `goodness' of the fit is more strongly dependent on the range of data used for fitting. For the data shown, the lowest density point is excluded from the fit, and the fitting range is $5\times10^9 < n <$ 8\10^9 cm^{-2}. The values of the relevant parameters are $\delta = 1.4\pm0.1$ and $n_c = 0.18\pm0.01 \times 10^{10}$ cm^{-2} at T=50 mK for sample A and $\delta = 1.5\pm0.1$ and $n_c = 0.28\pm0.02 \times 10^{10}$ cm^{-2} for sample B. These values of δ are close to the known 2D percolation exponent of 4/3.

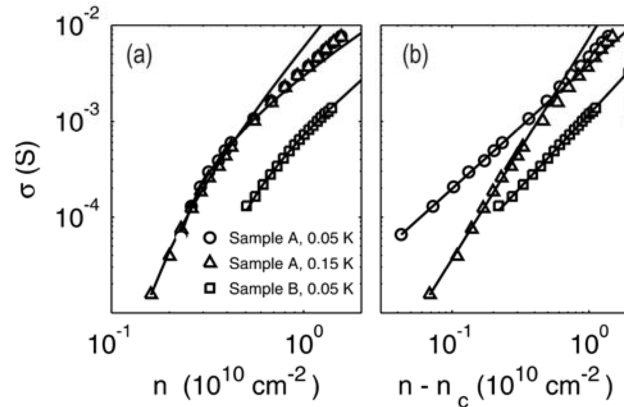

Figure 10. Experimental conductivity (symbols) fit to Eq. 1 (lines) for both Sample A and B as indicated in the legend. The same results are displayed as a function of n (2a) and $n - n_c$ (2b) to better show the low density region.

[3] A. L. Efros, Solid State Commun. 65, 1281 (1988); 70,253 (1989); D. Stau®er and A. Aharaony, *Introduction to Percolation Theory* (Taylor & Francis, London,1992); B. I. Shklovskii and A. L. Efros, *Electronic Properties of Doped Semicon-ductors* (Springer-Verlag, New Yorg, 1984).

Undoped electron-electron bilayers

Extending the processing techniques to fabricate completely undoped bilayers has been a significant challenge. The scheme that we choose to use is illustrated in Figure 11.

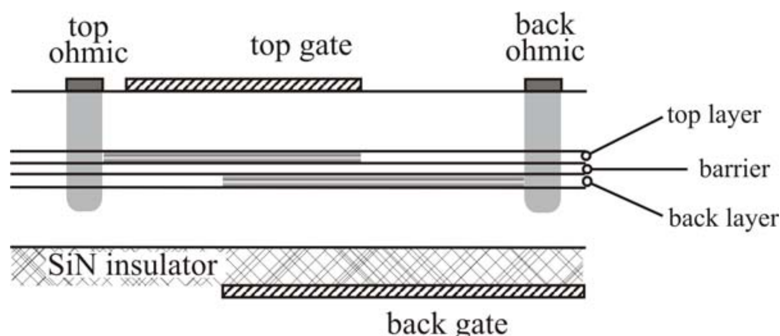

Figure 11. Cross sectional diagram of undoped bilayer structure. The top layer uses the self-aligned contact method described for the single layer undoped samples. The electric field for the back layer is also applied with an external gate, but the back gate is separated from the ohmic by both substract and SiN insulator. The regions where the gates overlap force the top and bottom layer into close proximity.

The GaAs/AlGaAs heterostructure consists of the following layers (from the top) 6 nm of n+ (top gate), 60 nm AlGaAs (x=0.3), 18 nm GaAs (top layer) 10 nm AlGaAs (x=0.55, barrier), 18 nm GaAs (bottom quantum well), 20 nm AlGaAs, and finally a cleaning superlattice and stop-etch layers near the substrate. First the top side of the undoped bilayer is processed using the same self-aligned contact procedure described above for the single layer undoped samples. Also on the top side are ohmic contacts for the back layer. After rapid thermal annealing, the contacts are ready for use. The sample is glued upside-down to a host substrate, and thinned using the EBASE (epoxy bond and stop etch) procedure developed at Sandia.[4] On the back side, an insulating layer is deposited, and then a gate that overlaps only the back contacts and the central interaction region. In the completed device, the top gate controls the density of the top layer, and the back gate controls the density of the back layer. Furthermore, we expect independent contacts.

The polarity of the carriers will depend on the material chosen for the ohmic contacts. If AuNiGe, then a positive gate voltage leads to electrons in the quantum well. If AuBe, then a negative gate voltage leads to holes in the quantum well. For a device with separate contacts, we can fabricate electron-electron, hole-hole or electron-hole bilayers.

The first attempt at fabricating this structure actually used a slightly modified version of the device shown in Figure 11 with n-type contacts. All of the contacts were self-aligned to the top gate, and the back gate overlapped all of the contacts. While the gates still controlled the top and back layers (respectively), no independent contacts are formed; i.e. each contact can be connected to both the top and the bottom layer. Magnetoresistance measurements are shown in Figure 13 for a fixed back gate voltage of 0.3 volts for several values of the top gate voltage. When the top gate voltage is 0, only the lower quantum well is populated with electrons. The

[4] M. V. Weckwerth, et al., Supperlatt. Microstruct. 20, 561 (1996).

minima in Figure 12a are periodic in 1/B, as expected for a single 2D system. In Figure 12b, the uniform 1/B oscillations are no longer obvious; here 2D systems of different density are present for both the top and bottom layers. A Fourier transform of the resistivity as a function of 1/B will yield the density of the two layers. Finally, in Figure 12c, the two layers have approximately equal density, and the uniform 1/B oscillations are recovered.

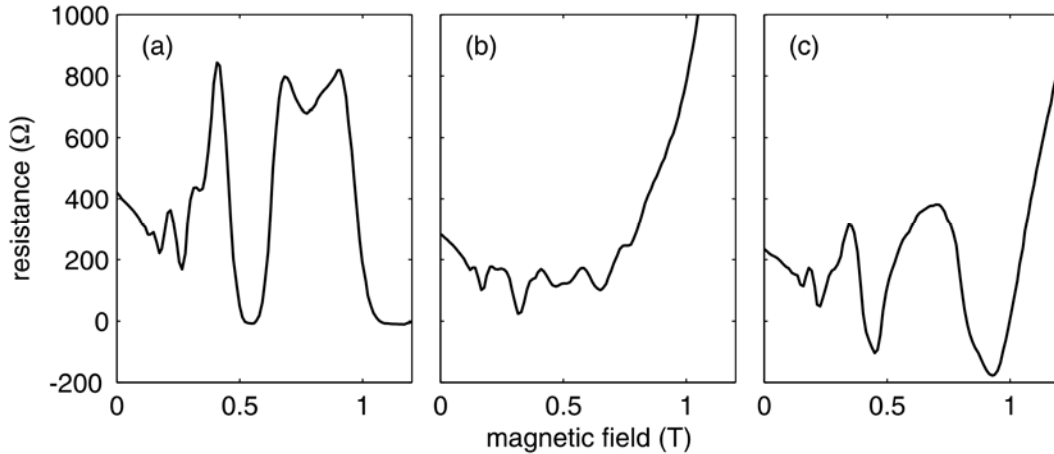

Figure 12. Magnetoresistance for different combinations of top gate voltage [(a) 0.0; (b) 0.08 and (c) 0.14 volts] for a fixed back gate voltage of 0.3 volts.

The density of both layers for the situation discussed above is summarized in Figure 13. The back gate voltage is fixed at 0.3 volts while the top gate voltage is varied, and the density is determined using Fourier transforms of the magnetoresistance. Initially, only the back 2D system is populated. As the top gate voltage is increased, we first measure the a top layer density above 0.05 volts, and higher voltages lead to a linear increase in the density of the top layer. The linear increase in density is the expected behavior as the gate and 2D system form a simple parallel plate capacitor. The density of the back layer has a small decrease as the top gate voltage is increased. One might initially guess that the back density would not change for a fixed back gate voltage. One the other hand, the density does depend on both the bandstructure and the compressibility of the top layer. Both of these effects are density dependent. The observed decrease in the density is not unreasonable.

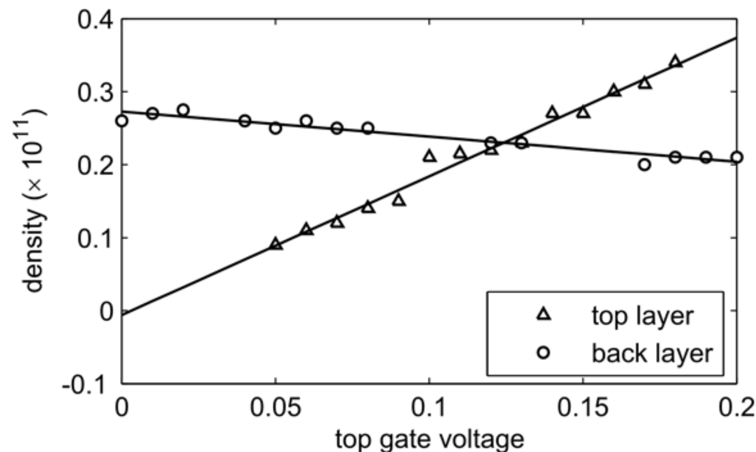

Figure 13. Density of the top and back layer for a fixed back gate voltage of 0.3 volts as the top gate is varied.

The magnetoresistance and density data show clear evidence that undoped bilayers function as advertised. This is the first ever demonstration of FET induced electrons on both the top and bottom layer in a bilayer structure. Extension of these techniques to include separate contacts and electron-hole bilayers should be straightforward.

Prospects for electron-hole bilayers and exciton condensation

With the demonstration that undoped bilayers can be fabricated and measured, we are very close to making and measuring electron-hole bilayers. Two changes are necessary: first modify the masks to allow for separate contacts as shown in Figure 12, and second to change one contact to p-type. These fairly straightforward processing changes are being tested as of the end of 2004, and should be successful. Once fabricated, transport in the electron-hole system will be tested for indications of exciton condensation and the resulting superconducting state.

Recent developments electron-electron and hole-hole bilayers at high magnetic field strongly suggest that exciton condensation physics in GaAs bilayers is present. In these studies[5], Coulomb drag and counterflow (oppositely directed currents in the upper and lower layer) are used to probe the novel quantum Hall state that is present when the lowest Landau layer is half-filled in each layer. This state can be describe both as quantum Hall ferromagnet or as exciton condensation of effective electron-hole quasiparticles. While the origin of this underlying state is due to many-body interactions between the layers, the description in terms of exciton condensation mimics that of electron-hole bilayers at zero magnetic field. These experiments indicate a high likelihood of observing exciton condensation at zero magnetic field for electron-hole bilayers. Of course, in the undoped electron-hole bilayer, many details will differ, but the realization of an electron-hole condensate as a platform for future experiments is a real possibility in the near future.

[5] M. Kellogg, *et al.*, Phys. Rev. Lett. 93, 036801 (2004); E. Tutoc, M. Shayegan, and D. A. Huse, Phys. Rev. Lett. 93, 036802 (2004).

Appendix I: List of refereed publications and presentations

Publications

1. M. P. Lilly, J. L. Reno, J. A. Simmons, I. B. Spielman, J. P. Eisenstein, L. N. Pfeiffer, K. W. West, E. H. Hwang, and S. Das Sarma, "Resistivity of dilute 2D electrons in an undoped GaAs heterostructure", Phys. Rev. Lett. **90**, 056806 (2003).
2. H. Noh, M. P. Lilly, D. C. Tsui, J. A. Simmons, E. H. Hwang, S. Das Sarma, L. N. Pfeiffer, and K. W. West, "Interaction corrections to two-dimensional hole transport in large r_s limit", Phys. Rev. B **68**, 165308 (2003).
3. S. Das Sarma, M. P. Lilly, E. H. Hwang, L. N. Pfeiffer, K. W. West, and J. L Reno, "2D metal-insulator transition as a percolation transition", submitted to Phys. Rev. Letters.
4. M. P. Lilly, E. Bielejec, J. A. Simmons and J. L. Reno, "Weak localization of dilute 2D electrons in undoped GaAs heterostructures", to appear in the Proceedings of the 27th International Conference on the Physics of Semiconductors (2004).

Invited Presentations

1. "Metallic behavior of the resistivity in dilute 2D electron systems", Condensed Matter Seminar at the University of Kentucky, September 2001.
2. "Metallic behavior of the resistivity in dilute 2D electron systems", Condensed Matter Seminar at the University of Massachusetts, April 2002.
3. "Metallic behavior of dilute 2D electron systems", Center for Advanced Studies Seminar at the University of New Mexico, October 2002.
4. "Metallic behavior of dilute 2D electron systems", Condensed Matter Seminar at the University of Texas, October 2002.
5. "Metallic behavior of dilute 2D electron systems", T11 Theory Group Seminar at Los Alamos National Laboratories, March 2003.
6. "Metallic behavior of dilute 2D electron systems", Electrical Engineering Seminar at Princeton University, July 2003.
7. "The contentious metallic state of two-dimensional electrons in semiconductors", Physics Colloquium, Texas A&M, September 2003.
8. "Metallic behavior of dilute 2D electron systems", Seminar at the National High Magnetic Field Laboratory, October 2003.
9. "The contentious metallic state of two-dimensional electrons in semiconductors", Condensed Matter Physics Seminar at the California Institute of Technology, October 2003.
10. "Exploring interactions and disorder using transport in low-dimensional semiconductor systems", Condensed Matter Seminar at the University of Maryland, November 2003.

11. “Coherence and Electron Interactions in the 2D metal-insulator regime”, Sixth International Conference on New Phenomena in Mesoscopic Systems, December 2003.
12. “Resistivity of ultra-low density two-dimensional electrons”, invited talk at the 2004 APS March meeting.

Distribution

1	MS 0601	John Reno, 01123
1	MS 0601	Denise Tibbetts, 01123
1	MS 0601	Roberto Dunn, 01123
1	MS 0601	Larry Stephenson, 01123
1	MS 0601	Wei Pan, 01123
1	MS 0601	Dan Barton, 01123
1	MS 0614	Wes Baca, 02522
1	MS 0614	Paul Butler, 02522
1	MS 1415	Michael Lilly, 01123
1	MS 1415	Edward Bielejec, 01123
1	MS 1415	John Seamons, 01123
1	MS 1415	Ken Lyo, 01123
1	MS 1421	Jerry Simmons, 01120
1	MS 1421	George Samara, 01120
1	MS 1427	Julia Phillips, 01100
1	MS 0123	LDRD Office, 1011
1	MS 9018	Central Technical Files, 8945-1
2	MS 0899	Technical Library, 9616
1	MS 0161	Patent and Licensing Office, 1150